Wave propagation and dispersion in microstructured wool felt

Anatoli Stulov and Dmitri Kartofelev

Abstract

On the basis of the experimental data of the piano hammers study the 1D nonlinear constitutive equation of the wool felt material is derived. A nonlinear partial differential equation with third order terms that takes into account the elastic and hereditary properties of a microstructured felt is used to study pulse propagation for the one-dimensional case. The leading physical dimensionless parameters are established and their importance for describing dispersion effects is discussed. The dispersion analysis of the linear problem is considered, and the range of the felt parameters which lead to the negative group velocity is determined. The initial value problem is considered and the numerical solution describing the strain wave evolution is provided. It is shown that the nonlinearity makes the front slope of a pulse steeper, which causes the eventual breaking of a pulse.

1 Introduction

Nowadays, there have been many studies of the mechanical behavior of materials with microstructure. This is the case of exploration of the oldest microstructured material, apparently, known to man. This remarkable material is the felt, the textile fabric made of wool. The felt is produced of randomized fibres, traditionally wool, or synthetic fibres that are tightly matted together. At present, the wool felt possessing a unique cellular structure is becoming increasingly popular and important as a resource material in various applications. For almost two hundred years the felt has been used in piano manufacturing. The felt pads are used as vibration isolation mounts under piano strings, the piano string dampers are made of wool felt, and of course, the felt made of wool is a unique and indispensable coating matter of piano hammers.

In this paper we briefly describe the model of felt proposed in [1]. There we derived a nonlinear constitutive equation of microstructured wool felt based on the experimental results of piano hammers testing. The discussion was centred around the boundary value problem that describes the propagation of deformation waves in the felt material. In this paper we focus our attention on the initial value problem, and consider the evolution of initial disturbance in the nonlinear microstructured wool felt. We provide also the detailed dispersion analysis of the linear problem, and show that for special values of physical parameters the waves with a negative group velocity may appear.

2 Wool felt model

To our knowledge the first study [2], which reports direct experimental research on the compression characteristics of the piano hammers, which are covered by the wool felt. Further experimental testing of piano hammers [3], confirms the main dynamical features of piano hammers: (a) the nonlinearity of the force-compression characteristics of the hammer, (b) the strong dependence of the hammer velocity on the slope of the loading curve, and (c) the significant influence of hysteresis, i.e. the loading and unloading processes of the hammer felt are not identical.

The first dynamical model of the piano hammer felt, which takes into consideration both the hysteresis of the force-compression characteristics and their dependence on the rate of felt loading was presented in [4]. The model is based on the assumption that the hammer felt (made of wool) is a microstructured material possessing history-dependent properties, i.e. a material with memory.

The constitutive equation of nonlinear microstructured wool felt is assumed in the form

$$\sigma(\epsilon) = E\epsilon^p(t). \tag{1}$$

Here σ is the stress, $\epsilon = \partial u/\partial x$ is the strain, u is the displacement, E is the Young's modulus, and p is the compliance nonlinearity exponent. Following Rabotnov [5], the constitutive equation of microstructured wool felt is derived by replacing the constant value of Young's modulus E in expression (1) by a time-dependent operator $E_d\left[1 - \mathcal{R}(t)*\right]$, where $*$ denotes the convolution operation, and the relaxation function is given by

$$\mathcal{R}(t) = \frac{\varepsilon}{\tau_0}\, e^{-t/\tau_0}, \quad 0 \leqslant \varepsilon \leqslant 1. \tag{2}$$

Here hereditary amplitude ε and relaxation time τ_0 are the hereditary parameters of wool felt.

This means that for the case of one-dimensional deformation and for any rate of loading the hysteretic felt material is defined by constitutive equation

$$\sigma(\epsilon) = E_d\left[\epsilon^p(t) - \mathcal{R}(t) * \epsilon^p(t)\right], \tag{3}$$

where constant E_d is the dynamic Young's modulus of the felt.

For very fast felt loading ($t \ll \tau_0$) from relation (3) follows the constitutive equation

$$\sigma(\epsilon) = E_d\epsilon^p(t), \tag{4}$$

and for slow loading ($t \gg \tau_0$) from relation (3) one shall obtain the constitutive equation

$$\sigma(\epsilon) = E_d(1-\varepsilon)\epsilon^p(t) = E_s\epsilon^p(t). \tag{5}$$

In each of these cases the loading and unloading of the felt follows the same path. The quantity $E_s = E_d(1-\varepsilon)$ is the static Young's modulus of the felt material.

The governing equation of motion, which describes the evolution of a wave (pulse) in the felt material is derived from classical equation of motion

$$\rho\frac{\partial^2 u}{\partial t^2} = \frac{\partial \sigma}{\partial x}, \tag{6}$$

where ρ is the density of the felt material.

Substituting (3) in Eq. (6), and eliminating the integral term leads to the equation of motion in terms of displacement u

$$\rho\frac{\partial^2 u}{\partial t^2} + \rho\tau_0\frac{\partial^3 u}{\partial t^3} - E_d\left\{(1-\varepsilon)\frac{\partial}{\partial x}\left[\left(\frac{\partial u}{\partial x}\right)^p\right] + \tau_0\frac{\partial^2}{\partial x \partial t}\left[\left(\frac{\partial u}{\partial x}\right)^p\right]\right\} = 0. \tag{7}$$

The dimensionless form of Eq. (7) one can obtained by using the non-dimensional variables, which are introduced by relations

$$u \Rightarrow u/l_0, \quad x \Rightarrow x/l_0, \quad t \Rightarrow t/\alpha_0, \tag{8}$$

where

$$\delta = 1-\varepsilon, \quad \alpha_0 = \tau_0/\delta, \quad l_0 = c_d\alpha_0\sqrt{\delta}, \quad c_d = \sqrt{E_d/\rho}, \quad c_s = c_d\sqrt{\delta}. \tag{9}$$

Thus Eq. (7) in terms of non-dimensional displacement variable $u(x,t)$ takes the following form

$$\left[(u_x)^p\right]_x - u_{tt} + \left[(u_x)^p\right]_{xt} - \delta u_{ttt} = 0, \tag{10}$$

and for the strain variable $\epsilon(x,t)$

$$(\epsilon^p)_{xx} - \epsilon_{tt} + (\epsilon^p)_{xxt} - \delta\epsilon_{ttt} = 0. \tag{11}$$

Several samples of felt pads made of the same material that is used in piano hammers manufacturing were subjected to the static stress-strain tests. The average value of the static Young's modulus of the pads was estimated to be $E_s = 0.6$ MPa. The average value of the felt density was $\rho = 10^3$ kg/m^3. Using the realistic values of hereditary parameters $\varepsilon = 0.96$ and $\tau_0 = 10$ μs, this results to the following values of material constants

$$\delta = 0.04, \quad E_d = 15 \text{ MPa}, \quad c_s = 25 \text{ m/s}, \quad c_d = 125 \text{ m/s}, \tag{12}$$

and the space and time units

$$l_0 = 6.25 \text{ mm}, \quad \alpha_0 = 0.25 \text{ ms}. \tag{13}$$

3 Linear case and dispersion relations

The linear approximation of the felt model demonstrates the significant characteristics of the wave propagation in the microstructured wool material. The given problem may be linearized in case of $p = 1$, and thus the linear form of the Eq. (11) is

$$\epsilon_{xx} - \epsilon_{tt} + \epsilon_{xxt} - \delta\epsilon_{ttt} = 0. \tag{14}$$

The fundamental solution of this equation has the form of traveling waves

$$\epsilon(x,t) = \hat{\epsilon}e^{ikx - i\Omega t}, \tag{15}$$

where i is the imaginary unit, k is the wavenumber, Ω is the angular frequency, and $\hat{\epsilon}$ is an amplitude. The dispersion law $\Phi(k,\Omega) = 0$ of Eq. (14) is defined by the relation

$$k^2 - \Omega^2 - ik^2\Omega + i\delta\Omega^3 = 0. \tag{16}$$

In the case of the initial value problem the general solution of Eq. (14) has following form

$$\epsilon(x,t) = \frac{1}{2\pi}\int_{-\infty}^{\infty} \chi(k)e^{ikx - i\Omega(k)t}dk, \tag{17}$$

where $\chi(k)$ is the Fourier-transform of initial disturbance

$$\chi(k) = \int_{-\infty}^{\infty} \epsilon(x,0)e^{ikx}dx. \tag{18}$$

The dependence $\Omega = \Omega(k)$ can be derived from dispersion relation (16). In general case $\Omega(k)$ is a complex quantity. In order to provide the dispersion analysis in the context of a initial value problem we rewrite the frequency $\Omega(k)$ in the form

$$\Omega(k) = \omega(k) + i\mu(k), \tag{19}$$

where $\omega = \mathrm{Re}(\Omega)$ and $\mu = \mathrm{Im}(\Omega)$. Using this notation, expression (15) can be rewritten as follows

$$\epsilon(x,t) = \hat{\epsilon}e^{ikx - i\omega t + \mu t} = e^{\mu t}\hat{\epsilon}e^{ikx - i\omega t}. \tag{20}$$

From this relation (20), it is evident that for negative values of μ it acts as an exponential time decay constant for the spectral components of the initial disturbance. On the other hand if $\mu(k) > 0$ then the amplitudes of spectral components grow exponentially in time during the wave evolution. In this case the solution of linear equation (14) becomes unstable for $t \gg 0$.

4 Dispersion analysis

In order to study the initial value problem one needs to solve the dispersion relation (16) against the wavenumber k. Taking into account (19), the dispersion relation (16) takes the following form

$$k^2 - ik^2\omega - \omega^2 + i\delta\omega^3 + k^2\mu - 2i\omega\mu - 3\delta\omega^2\mu + \mu^2 - 3i\delta\omega\mu^2 + \delta\mu^3 = 0. \tag{21}$$

Splitting (21) into the real and imaginary parts on can obtain the system of equations

$$\begin{cases} k^2(1+\mu) - 3\delta\omega^2\mu + \delta\mu^3 - \omega^2 + \mu^2 = 0 \\ \delta\omega^3 - 3\delta\omega\mu^2 - 2\omega\mu - k^2\omega = 0 \end{cases}. \tag{22}$$

Solving this system of equations with respect to ω and μ one can obtain nine sets of solutions in total. Among these, there is only one physically reasonable solution, which satisfies the conditions $\forall\omega \in \mathbb{R}$, $\forall\mu \in \mathbb{R}$, and $\mu \leqslant 0$

$$\begin{cases} \omega = \frac{\sqrt{6}}{12\delta S}\sqrt{\sqrt[3]{2}S^4 - 4S^2(1-3k^2\delta) + 2\sqrt[3]{4}(1-3k^2\delta)^2} \\ \\ \mu = \frac{1}{12\delta S}\left[\sqrt[3]{4}S^2 - 4S + 2\sqrt[3]{2}(1-3k^2\delta)\right] \end{cases}. \tag{23}$$

Here

$$S = \sqrt[3]{2 - 9k^2\delta(1-3\delta) + 3k\delta\sqrt{3Q}}, \tag{24}$$

and

$$Q = 4k^4\delta - k^2(1 + 18\delta - 27\delta^2) + 4. \tag{25}$$

It can be shown that four distinct solutions with respect to ω and μ of this dispersion relation exist depending on the value of the parameter δ. These four sets of values are: i) $\delta = 0$; ii) $0 < \delta \leqslant 1/9$; iii) $1/9 < \delta < 1$; iv) $\delta = 1$. Below we will thoroughly examine these four cases, and explain the differences between them in detail.

4.1 Dispersion analysis, case $\delta = 0$

If material parameter $\delta = 0$ then the system of equations (22) takes the form

$$\begin{cases} k^2 - \omega^2 + k^2\mu + \mu^2 = 0 \\ k^2\omega + 2\mu\omega = 0 \end{cases}. \tag{26}$$

Solving with respect to ω and μ gives two different solutions of system (26). The first one is

$$\begin{cases} \omega = k\sqrt{1 - k^2/4} \\ \mu = -k^2/2 \end{cases}. \tag{27}$$

This solution is defined for the following values of wavenumber $\forall k \in \{k \mid 0 \leqslant k \leqslant k_\alpha\}$, where the value of k_α can be determined as follows

$$1 - \frac{k^2}{4} = 0 \Rightarrow k_\alpha = 2. \tag{28}$$

The second solution of system(26) has the form

$$\begin{cases} \omega = 0 \\ \mu = -k^2/2(1 \pm \sqrt{1 - 4/k^2}) \end{cases}, \tag{29}$$

and it is defined for values of wavenumber $k > 2$. Although, this solution satisfies the conditions $\forall\omega \in \mathbb{R}$, $\forall\mu \in \mathbb{R}$, and $\mu \leqslant 0$, the careful analysis shows that this solution (29) must be rejected. In fact, this solution leads to the problem that the strain field defined by the integral form (17) dos not satisfy the Sommerfeld radiation condition.

The corresponding dispersion curves of solution (27) are plotted in Fig. 1. The function $\mu(k) = \mathrm{Im}(\Omega(k))$ is negative for all non-negative k, which according to expression (20) means that this wave process is decaying with progression of time.

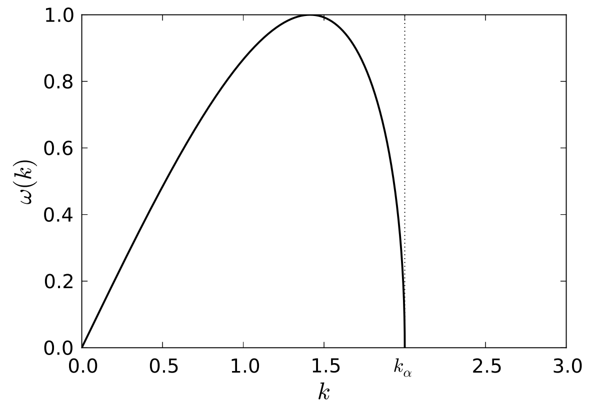

Figure 1: Dispersion relations $\omega(k)$ and $\mu(k)$ for value of parameter $\delta = 0$.

From the careful study of the dispersion curves on Fig. 1, one can notice that dispersion curve sets clear restrictions on possible frequencies and wavenumbers that are allowed to propagate inside the felt material. The allowed frequencies span from 0 to 1, and the allowed wavenumbers span from 0 to 2.

The phase velocity which is defined as $v_{\mathrm{ph}}(k) = \omega/k$ in this case amounts to a following value

$$v_{\mathrm{ph}} = \sqrt{1 - k^2/4}, \quad \forall k \in \{k \mid 0 \leqslant k \leqslant k_\alpha\}, \tag{30}$$

and has the same restrictions on the values of wavenumber k.

The group velocity which is defined as $v_{\mathrm{gr}}(k) = d\omega/dk$ in this case amounts to a following value

$$v_{\mathrm{gr}} = \frac{2 - k^2}{\sqrt{4 - k^2}}, \quad \forall k \in \{k \mid 0 \leqslant k < k_\alpha\}. \tag{31}$$

The corresponding phase and group velocities are plotted on Fig. 2. One can see that $v_{\mathrm{ph}}(k) > v_{\mathrm{gr}}(k)$ for all allowed wavenumbers $0 < k \leqslant k_\alpha$, which means that dispersion type is the normal dispersion. It is interesting to note that the group velocity of some wave components are allowed to become negative for $\sqrt{2} < k < k_\alpha$. Most likely no exotic behaviour usually associated with negative group velocity can be observed in the actual wave process because, as was shown above, the wave components that have larger values of k will decay very fast, and thus the low frequency components, that have the positive group velocity, will prevail.

4.2 Dispersion analysis, case $0 < \delta \leqslant 1/9$

The solution (23), which satisfies the conditions $\forall\omega \in \mathbb{R}$, $\forall\mu \in \mathbb{R}$, and $\mu \leqslant 0$ in case of $0 < \delta \leqslant 1/9$ is valid only for specific interval of wavenumber $\forall k \in \{k \mid 0 < k \leqslant k_\alpha \wedge k_\beta \leqslant k < \infty\}$. Here the values of wavenumbers k_α and k_β can be determined as follows

$$k_\alpha = \frac{1}{2\sqrt{2}}\sqrt{18 - 27\delta - \frac{1 - \sqrt{(1-\delta)(1-9\delta)^3}}{\delta}}, \tag{32}$$

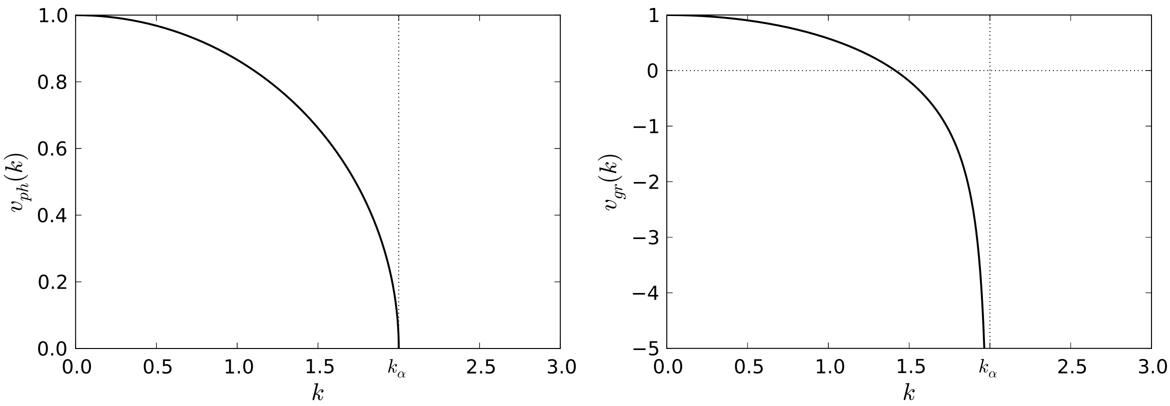

Figure 2: Phase and group velocities as functions of wavenumber k for the case of parameter $\delta = 0$.

$$k_\beta = 1/\sqrt{3\delta}, \tag{33}$$

Table 1: Values of k_α and k_β

	$\delta = 0$	$\delta = 1/9$
k_α	2	$\sqrt{3}$
k_β	∞	$\sqrt{3}$

It stands that relationship between the values of k_α and k_β is always that $k_\alpha \leqslant k_\beta$. k_α and k_β signify the beginning and the end values of band-gap region. Wave components that are in between k_α and k_β are not allowed to propagate in the felt material (which is to say that they decay with infinite exponential decay constant). If one compares this case $(0 < \delta \leqslant 1/9)$ with the previous $(\delta = 0)$, one realizes that they are complimenting each other (compare Table 1). It can be said that previous case has also a band-gap region on infinite width extending from k_α to infinity, as it is evident from the analysis of the current case.

Fig. 3 shows dispersion curves for various values of the parameter δ in the interval $(0 < \delta \leqslant 1/9]$. With the growth of the value of the parameter δ width of the band-gap region becomes narrower and the value of the exponential decay constant becomes progressively smaller especially for higher frequency wave components (larger k values).

The limits for dispersion relation are

$$\lim_{k \to \infty} \omega = \infty, \qquad \lim_{k \to \infty} \mu = -\frac{1-\delta}{2\delta} = \mu_\alpha. \tag{34}$$

The decay constant values for low values of wavenumbers $k < k_\alpha$ are smaller (as a rule) compared to previous case $(\delta = 0)$ but overall qualitative behaviour of the dispersion relation in this region is exactly the same. Careful study of the dispersion relation for the wavenumbers $k > k_\beta$ reveals that exponential decay values μ become more or less unchanging starting right after the band-gap region ends and also that the values of the decay constants for $k > k_\beta$ are enormous.

To conclude the comparison of the current case with the previous one, although at first glance dispersion curves look very different, the underlying wave propagation process is most likely exactly the same. How so? The explanation lies in the fact that the values of the decay constants for new additions of the dispersion curves compared to the first case, starting after the end of the band-gap region, are enormous. These wave components will decay long before they can produce

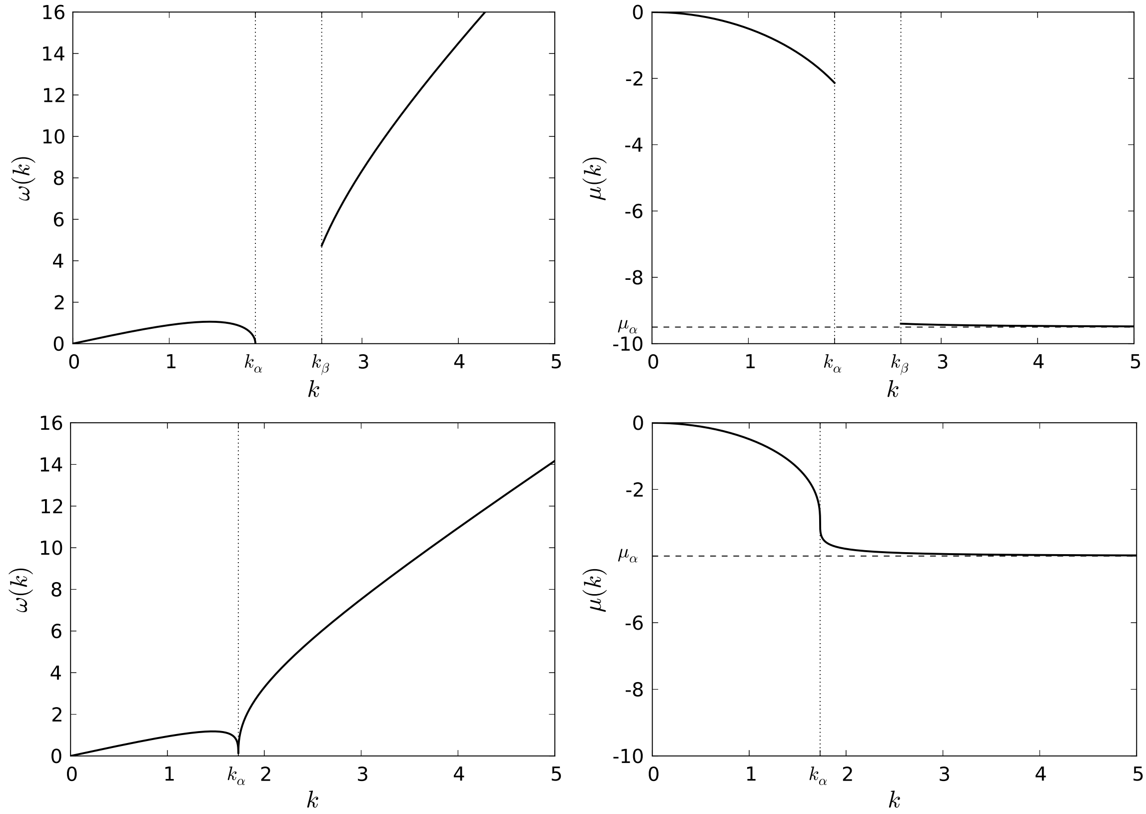

Figure 3: Dispersion relations $\omega(k)$ and $\mu(k)$ for values of parameter $\delta = 0.05$ (top row), and $\delta = 1/9$ (bottom row).

any noticeable difference in the wave process compared with the first case. That conclusion can be verified with ease by conducting the numerical experiments.

The phase velocity for the current case is obtained from (23) as

$$v_{\text{ph}} = \frac{\sqrt{6}}{12\delta k S}\sqrt{\sqrt[3]{2}S^4 - 4S^2(1-3k^2\delta) + 2\sqrt[3]{4}(1-3k^2\delta)^2}. \tag{35}$$

The group velocity can be calculated by taking derivative $v_{\text{gr}}(k) = d\omega/dk$. The resulted analytical expression is too long thus it will not be presented here. The same band-gap restriction applies for the phase and group velocities as applied for the dispersion relation. It means that

$$\exists v_{\text{ph}},\ \exists v_{\text{gr}}\ \forall k \in \{k \mid 0 < k \leqslant k_\alpha \wedge k_\beta \leqslant k < \infty\}. \tag{36}$$

Figure 4 shows the phase and group velocities plotted against the wavenumber k. As in previous case here we have $c_{\text{ph}}(k) > c_{\text{gr}}(k)$ for the region where $k < k_\alpha$, and this means that the dispersion type is normal. The limit of these velocities are

$$\lim_{k\to\infty} v_{ph} = \lim_{k\to\infty} v_{gr} = \frac{1}{\sqrt{\delta}} = \delta_\alpha. \tag{37}$$

For the wavenumbers $k > k_\beta$ $c_{\text{ph}}(k) < c_{\text{gr}}(k)$, and this means that type of dispersion after the band-gap region is the anomalous dispersion. But as it is mentioned above this does not guarantee that one could observe effects usually associated with the anomalous dispersion in the felt because of the extreme decay associated with that part of the dispersion curve.

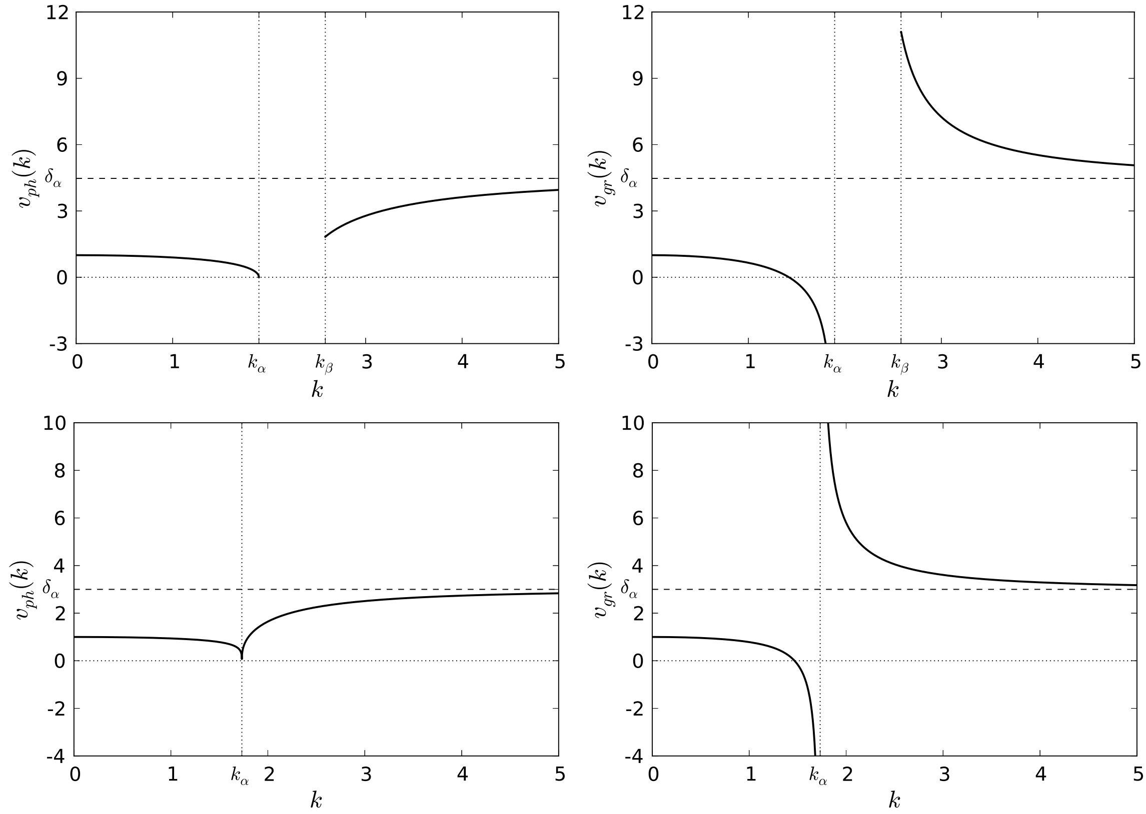

Figure 4: Phase and group velocities for case $0 < \delta \leqslant 1/9$ plotted as a function of wavenumber k for values of parameter $\delta = 0.05$ (top row), and $\delta = 1/9$ (bottom row).

Here, as in the previous case the negative group velocity are allowed for the some wave components. The negative values of the group velocity exist if the value of material parameter δ lies in the interval [0, 0.134]. That means for the entire interval of the current case. Again we conclude that no exotic physical effect will arise from this fact, due to of a relatively big decay associated with these wave components.

4.3 Dispersion analysis, case $1/9 < \delta < 1$

The solution (23), which satisfies the conditions $\forall\omega \in \mathbb{R}$, $\forall\mu \in \mathbb{R}$, and $\mu \leqslant 0$ in case of $1/9 < \delta < 1$ is valid for all non-negative values of the wavenumber k. This means that no band-gap region exist in this case and that is the main difference between this and the previous cases.

The phase and group velocities can be calculated using the results from the previous case but without the need to apply restrictive band-gap.

Figure 5. shows the dispersion curves for the current case. No band-gap is present and one can notice that as the parameter δ becomes larger the dispersion curve $\omega(k)$ becomes more and more similar to the dispersion curve on non-dispersive media ($\omega(k) = k$). The decay values of the wave components are smaller compared to the previous cases. In Fig. 6 the phase and group velocities are plotted against the values of wavenumber k. Similarly to the previous case the regions of normal ($c_{\mathrm{ph}}(k) > c_{\mathrm{gr}}(k)$) and anomalous ($c_{\mathrm{ph}}(k) < c_{\mathrm{gr}}(k)$) dispersion can be distinguished. From numerical experiments it follows that although the decay values for higher frequencies (bigger k values) are much smaller then in all the previous cases effects of the anomalous dispersion are not observable (see Fig. 7 and 8). Nether are effect associated with the negative group velocity. The limit curves, which are shown in Fig. 5, and Fig. 6 by dashed lines are defined by parameters μ_α, and δ_α that

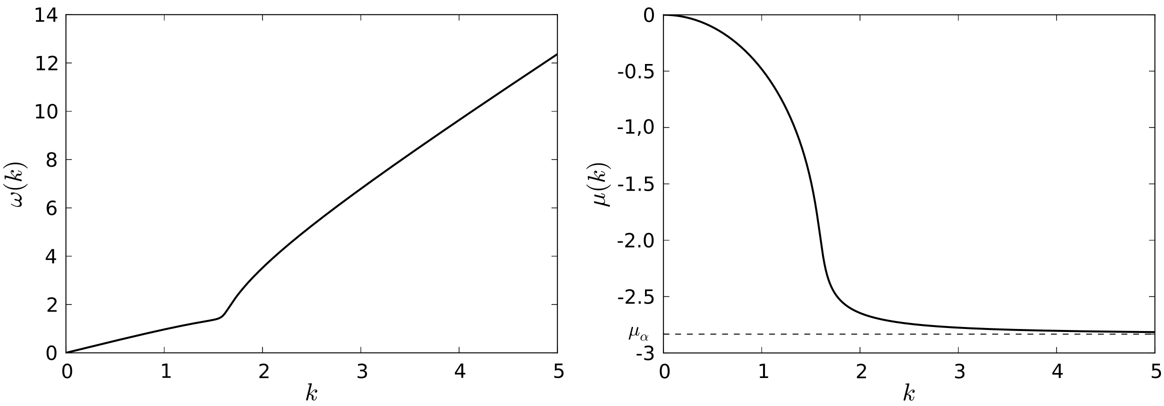

Figure 5: Dispersion relations $\omega(k)$ and $\mu(k)$ for value of parameter $\delta = 0.15$.

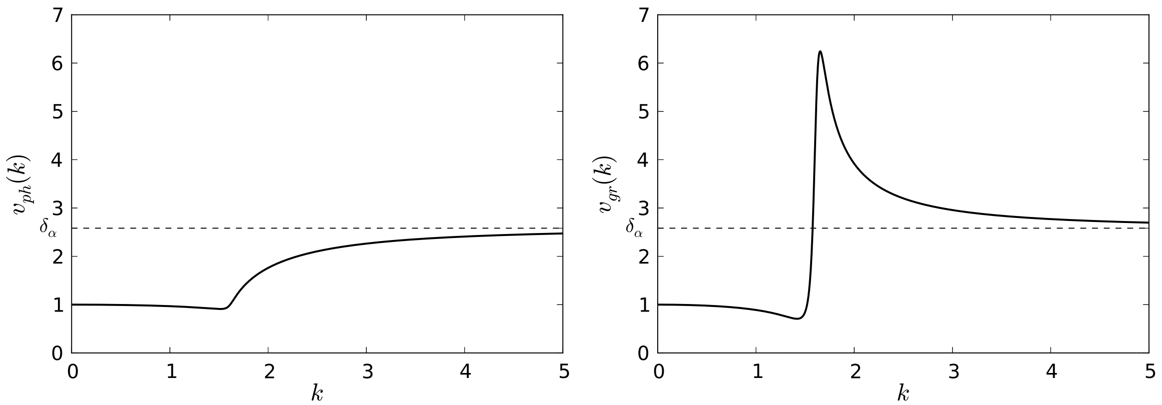

Figure 6: Phase and group velocities for case $0 < \delta < 1$ plotted as a function of wavenumber k for values of parameter $\delta = 0.15$.

are determined by relations (34) and (37).

4.4 Dispersion analysis, case $\delta = 1$

The solution (23), in this case is

$$\begin{cases} \omega = k \\ \mu = 0 \end{cases}, \tag{38}$$

and this result means that if the parameter $\delta = 1$, then the solution of the dispersion relation (16) with respect to ω has a real valued solution $\omega(k) = k$. It is well known that this case represents the non-dispersive solution and obviously in this case no decaying wave components exist. In addition, it is simple to obtain that for the linear case ($p = 1$) the felt equation in the form (41) amounts to an ordinary wave equation

$$\epsilon_{tt} = \epsilon_{xx}. \tag{39}$$

The corresponding phase velocity in this case is $v_{\text{ph}}(k) = k/k = 1$, and the corresponding group velocity is $v_{\text{gr}}(k) = d(k)/dk = 1$.

5 Numerical solution of initial value problem

5.1 Numerical scheme

The goal of this study is to analyze the evolution of the one dimensional strain wave inside the felt material. This calls for the solution of the initial value problem of the Eq. (11). A initial strain distribution is selected in the following form

$$\epsilon(x,0) = A\exp[-(\alpha x)^2], \tag{40}$$

where A defines the maximum of amplitude of the distribution, and α is the space parameter.

The solution of the initial vale problem is obtained numerically, by using finite difference method. Instead of Eq. (11) we use a more suitable form of this equation that can be obtained by integrating it over time.

$$\epsilon_{tt} = (\epsilon^p)_{xx} - \varepsilon \int_0^t (\epsilon^p)_{xx} e^{\xi - t} d\xi. \tag{41}$$

This integral form is more suitable for finite difference scheme. Integration in this expression will be approximated by applying trapezoidal rule.

Discrete time and space domains are used. Time domain is divided into n discrete parts using uniform grid with step size $\Delta t = t_{j+1} - t_j$ where $j = 1, \ldots, n$ ($j \in \mathbb{Z}$) and space domain is divided into m discrete parts using uniform step size $\Delta x = x^{i+1} - x^i$ where $i = 1, \ldots, m$ ($i \in \mathbb{Z}$). Lower indexes will be used to denote time and upper indexes will be used to denote space steps. For example $\epsilon_j^i \equiv \epsilon(i\Delta x, j\Delta t)$.

Second order space derivative of quantity $(\epsilon^p)_{xx}$ in equation (41) is

$$(\epsilon^p)_{xx} = p(p-1)\epsilon^{p-2}(\epsilon_x)^2 + p\epsilon^{p-1}\epsilon_{xx}, \tag{42}$$

here following finite difference approximations for the parts of this expression are used

$$\epsilon_x \approx \frac{1}{2\Delta x}(\epsilon_j^{i-1} - \epsilon_j^{i+1}), \tag{43}$$

$$\epsilon_{xx} \approx \frac{1}{\Delta x^2}(\epsilon_j^{i-1} - 2\epsilon_j^i + \epsilon_j^{i+1}), \tag{44}$$

$$\epsilon_{tt} \approx \frac{1}{\Delta t^2}(\epsilon_{j-1}^i - 2\epsilon_j^i + \epsilon_{j+1}^i), \tag{45}$$

it follows that quantity

$$(\epsilon^p)_{xx} \approx \frac{1}{\Delta x^2}\left[\frac{1}{4}p(p-1)(\epsilon_j^i)^{p-2}(\epsilon_j^{i-1} - \epsilon_j^{i+1})^2 + p(\epsilon_j^i)^{p-1}(\epsilon_j^{i-1} - 2\epsilon_j^i + \epsilon_j^{i+1})\right]. \tag{46}$$

After combining above mentioned, explicit finite difference scheme for approximating solution of the equation (41) for all discrete grid points i and j takes form

$$\epsilon_{j+1}^i = \frac{\Delta t^2}{\Delta x^2}\left(b_j^i - \varepsilon e^{-j\Delta t} I_j^i\right) + 2\epsilon_j^i - \epsilon_{j-1}^i, \tag{47}$$

here

$$b_j^i = 0.25p(p-1)(\epsilon_j^i)^{p-2}(\epsilon_j^{i-1} - \epsilon_j^{i+1})^2 + p(\epsilon_j^i)^{p-1}(\epsilon_j^{i-1} - 2\epsilon_j^i + \epsilon_j^{i+1}), \tag{48}$$

$$I_j^i = I_{j-1}^i + \frac{(b_{j-1}^i e^{(j-1)\Delta t} + b_j^i e^{j\Delta t})}{2}\Delta t. \tag{49}$$

Quantity I corresponds to the integration part of the equation (41). Exponential functions will be approximated using Maclaurin expansion in the form

$$e^{\xi} \approx 1 + \xi + \frac{\xi^2}{2} + O(\xi^3), \tag{50}$$

this will be done in order to assure same order of accuracy between finite difference approximation and the exponential functions for example in (47). In addition this will help to sustain stability of the numerical solution.

The presented finite difference method is better suited for solving linear problems (in our case $p = 1$), but this particular FDM scheme can produce stable solution also for the nonlinear cases.

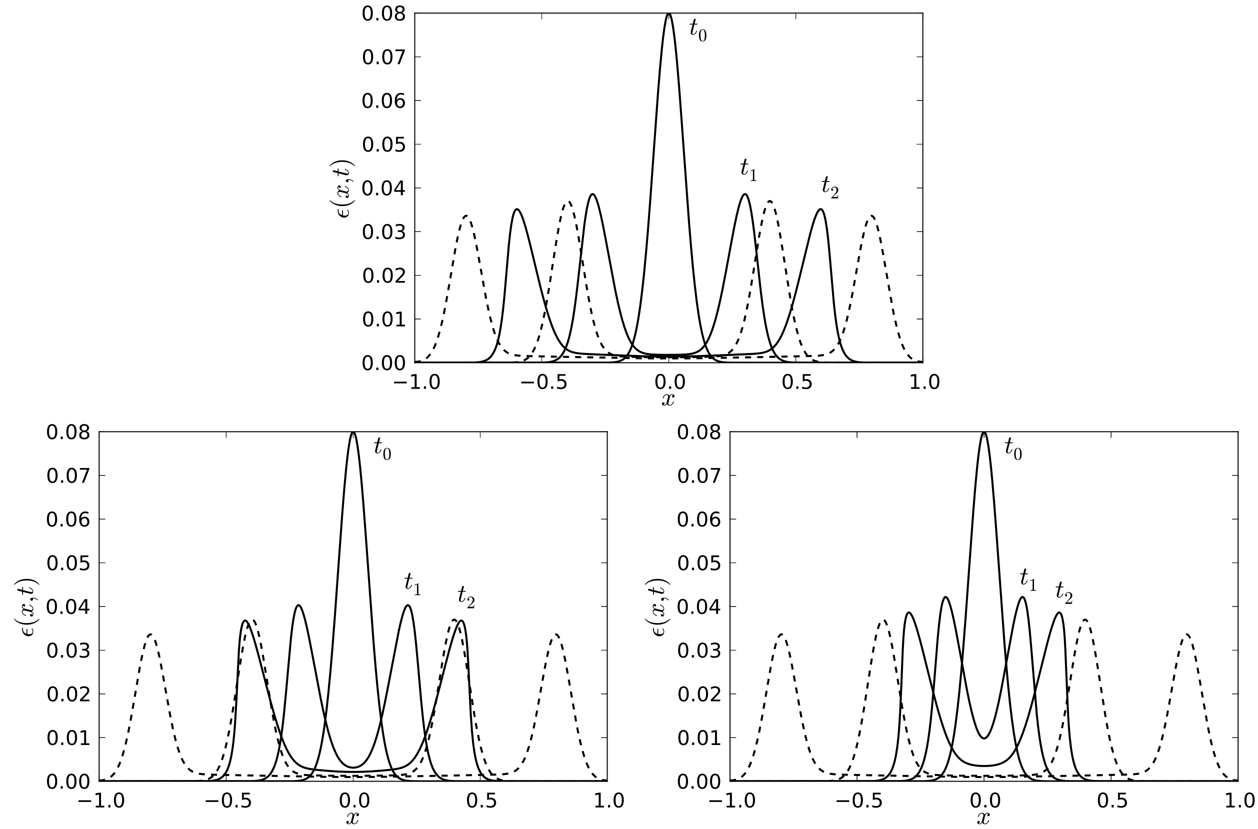

Figure 7: Nonlinear evolution of the initial disturbance ($A = 0.08$, $\alpha = 12$, $\delta = 0.5$) for three sequential time moments $t_0 = 0$, $t_2 = 0.4$ and $t_3 = 0.8$, varying the nonlinear parameter p: $p = 1.5$ (top row), $p = 2.0$ (bottom row left), and $p = 2.5$ (bottom row right).

5.2 Parameter p influence

In this section the effects of the nonlinearity of the wool felt model on the wave evolution are considered. We examine the influence of the nonlinearity parameter p, on the changing of the wave form during its propagation in the felt material.

Figure 7 shows numerical solution of the initial value problem (40), (41). The solution of the problem is presented for three sequential time moments, and for three different values of the nonlinearity parameter p. In these examples the amplitude $A = 0.08$, and parameter $\delta = 0.5$ and $\alpha = 12$ are constants for all cases presented.

In Fig. 7 it is possible to see that the front of the pulse becomes steeper as the pulse propagates through the felt material. This pulse steepening increases with the growth of the value of parameter

p. It means that the group velocity is greater than the phase velocity. This phenomenon confirms our conclusion that the felt is a material with anomalous dispersion.

5.3 Amplitude A influence

The effect of the initial pulse amplitude A on a pulse evolution in the felt material is presented in Fig. 8. The numerical solution is presented for three sequential time moments, and for three different values of the initial amplitude A of the initial value problem (40), (41). It is possible to see that a forward-facing slope of the pulse is strongly dependent on the pulse amplitude A. Accumulation of this effect results in the eventual pulse breaking. This means that the shock wave will be formed. To simulate this phenomenon, our numerical scheme must be adjusted to the purpose of description of propagation of discontinuities on the wave front. A detailed analysis of this problem is in progress. The progressive forward leaning of the propagating pulse is related to the nonlinear features of the

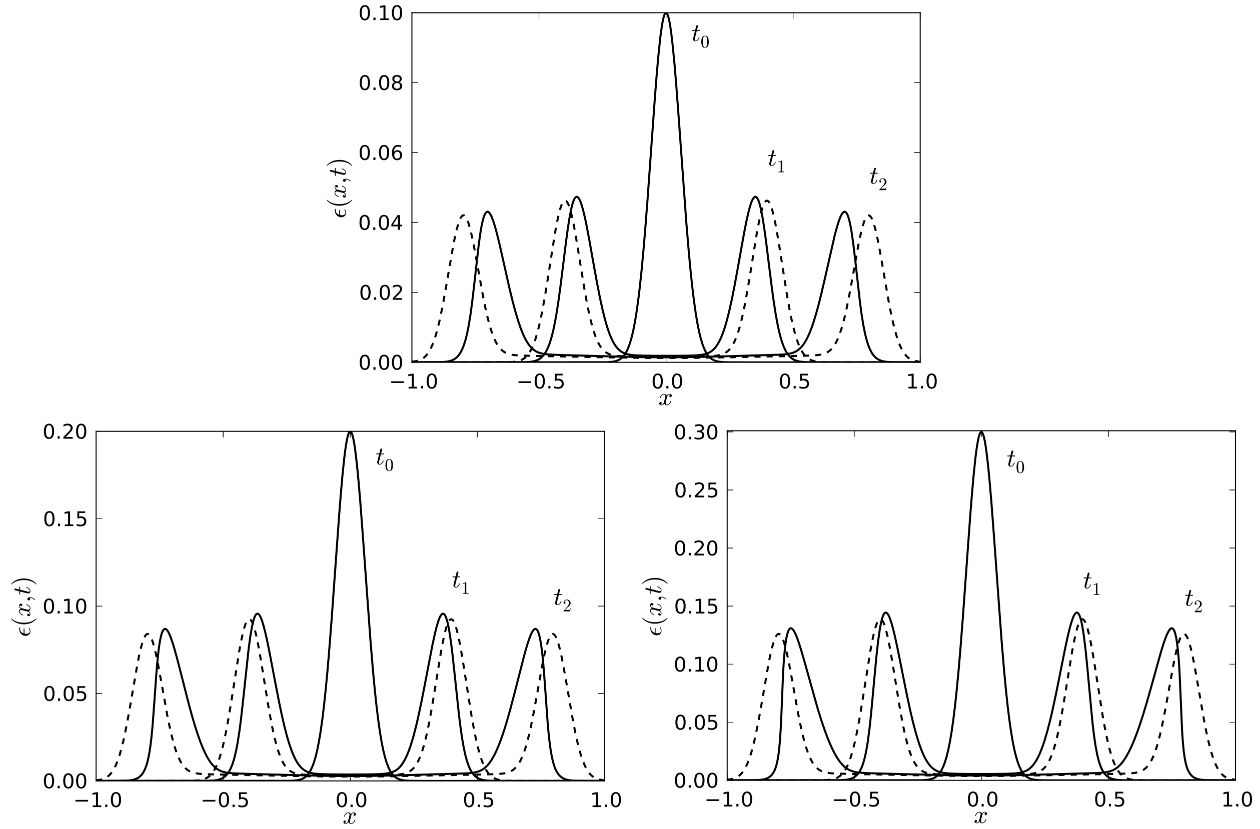

Figure 8: Nonlinear evolution of the initial disturbance ($\alpha = 12$, $\delta = 0.5$, $p = 1.25$) for three sequential time moments $t_0 = 0$, $t_2 = 0.4$ and $t_3 = 0.8$, varying the amplitude A: $A = 0.1$ (top row), $A = 0.2$ (bottom row left), and $A = 0.3$ (bottom row right).

felt material, and increases with the increasing of the amplitude of the initial disturbance.

6 Conclusions

The dispersion analysis of the linear problem in the form (14) was considered, and we have demonstrated that in the case of large values of hereditary amplitude ($\varepsilon > 0.865$) of the felt material the negative group velocity can be identified. This phenomena was discussed also in [6], and the range of the felt parameters which lead to the negative group velocity in microstructured materials is determined. In the case of a felt-type material, the emergence of negative group velocity depends on the hereditary parameters ε and relaxation time τ_0, which is related to viscoelastic features of such a microstructured material.

The initial value problem is considered and the numerical solution describing the strain wave evolution is provided. It is shown that the nonlinearity makes the front slope of a pulse steeper, which causes the eventual breaking of a pulse.

It was shown that the wool felt as a microstructured material has very strong damping effect on any pulse propagating through it. In conclusion the felt material can be considered strongly dissipative and normally dispersive media for almost all of the values of the material parameter δ.

Acknowledgements

This research was supported by the EU through the European Regional Development Fund, and by the Estonian Ministry of Education and Research (SF 0140077s08).

References

[1] Kartofelev, D., Stulov, A.: Propagation of deformation waves in wool felt. ACTA Mechanica, (2014) (submitted).

[2] Yanagisawa, T., Nakamura, K.: Dynamic compression characteristics of piano hammer. Trans. of Musical Acoust. Technical Group Meeting of Acoust. Soc. Jpn. **1**, 14–18 (1982).

[3] Stulov, A.: Experimental and computational studies of piano hammers. Acta Acoustica united with Acoustica, **91**, 1086–1097 (2005).

[4] Stulov, A.: Hysteretic model of the grand piano hammer felt. J. Acoust. Soc. Am. **97**, 2577–2585 (1995).

[5] Rabotnov, Yu. N.: Elements of hereditary solid mechanics, Chap. 17. Moscow: MIR Publishers (1980).

[6] Peets, T., Kartofelev, D., Tamm, K., and Engelbrecht J.: Waves in microstructured solids and negative group velocity. EPL - A Letters Journal Exploring the Frontiers of Physics, vol. 103, no. 1, pp. 16001-p1 - 16001-p6.